

國立臺灣大學生物資源暨農學院生物機電工程學系



碩士論文

Department of Biomechatronics Engineering

College of Bioresources and Agriculture

National Taiwan University

Master Thesis

利用卷積神經網路建立雞隻張嘴行為、散佈程度與活動

力之預警系統

Early Warning System for Open Beak Behavior, Spatial

Dispersion, and Movement of Chickens Using

Convolutional Neural Networks

陳柏霖

Bo-Lin Chen

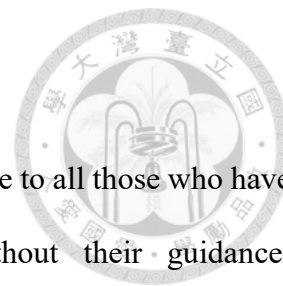
指導教授：郭彥甫 博士

Advisor: Yan-Fu Kuo, Ph.D.

中華民國 112 年 6 月

June, 2023

ACKNOWLEDGEMENTS



I would like to take this opportunity to express my heartfelt gratitude to all those who have supported and assisted me during my master project. Without their guidance, encouragement, and contributions, this research would not have been possible. Firstly, I extend my deepest appreciation to Professor Yan-Fu Kuo, my main research advisor. His meticulous guidance, unwavering support, and valuable suggestions have been instrumental in shaping the direction of my research. I am truly grateful for his expertise and dedication. Secondly, I would also like to extend my thanks to Dino and Jack, who have been with me throughout the same period. Their insightful suggestions and feedback have been tremendously valuable. Although we lost Dino on November 20, 2022, his impact on my work continues to resonate. I will always cherish his contributions and be deeply missed. Thirdly, I would also like to extend my thanks to the members of Lab203, namely Kent, Mao-Xiang, Hong-Yang, Hseuh-Hung, Kuan-Ting, Kim, Yihsin, Yun, Jensen, Karl, Ting-hui, and Dawson. Their assistance, collaboration, and insightful discussions have significantly enriched my work. Lastly, I would like to express my sincere appreciation to my family. Their unwavering support, encouragement, and love have been my constant source of motivation and strength. I am forever grateful for their understanding and belief in me, especially during the most challenging times.

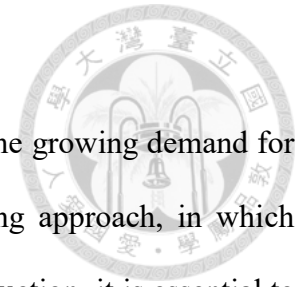
摘要



雞肉在全球蛋白質供應鏈中佔有重要地位，隨著市場需求不斷增長，採取集約化飼養方式，將大量雞隻放置於同一環境中已經成為常態。在這種情況下，對於雞群生長狀態的持續監控成為確保產量穩定的關鍵要素。傳統上，雞隻的張嘴行為、散佈程度和活動力都是由人工監控，然而這種方式不僅耗時且耗力，並且難以實現即時異常偵測。為解決上述問題，本研究提出了預警系統，藉由量化雞隻的張嘴行為、散佈程度與活動力，進行監測。預警系統由多台嵌入式設備、Wi-Fi 網狀網路、雞隻張嘴偵測模型和雞隻追蹤模型組成。嵌入式系統包含鏡頭分別安裝在雞舍的支柱和橫樑上，從側視和俯視角度捕捉雞隻的影像，再透過 Wi-Fi 網狀網路傳送到雲端伺服器儲存。雞隻張嘴偵測模型用於偵測側視影像中的雞隻頭部，並將其分為兩類：張嘴與未張嘴。透過雞隻張嘴偵測模型偵測結果，可計算張嘴雞隻佔所有偵測到的雞隻比例。雞隻偵測與追蹤模型用於偵測俯視影像中的雞隻位置，並利用最近臨演算法與 Bytetrack 演算法，分別計算雞隻的散佈程度與活動力。經過量化完成之張嘴雞隻比例、散佈程度與活動力，分別使用平均值與標準差、自回歸整合移動平均 (ARIMA) 的 95%信賴區間、以及季節性自回歸整合移動平均模型含有外生變數 (SARIMAX) 的 95%信賴區間來確定其安全區間。當數值超出該安全區間的數值即被認為是警告。在結果方面，雞隻張嘴偵測模型在雞隻頭部的分類與偵測上，整體平均精度達到 91.3%。雞隻偵測與追蹤模型在雞隻偵測上，平均精度達到 95.8%，再多目標追蹤準確率達到 89.5%。此外，在自回歸整合移動平均模型的平均絕對百分比誤差達到 3.44%，而季節性自回歸整合移動平均模型含有外生變數的平均絕對百分比誤差達到 13.76%。本研究提供了一個完整且全自動化的預警系統，旨在為雞場管理員提供實時且有效的數據支援，以便他們能更有效地管理雞場。

關鍵詞：嵌入式系統、最近臨演算法、Bytetrack 演算法、深度學習

ABSTRACT



Chicken is a major source of dietary protein worldwide. To meet the growing demand for chicken meat, chickens are usually raised using intensive farming approach, in which thousands of chickens are housed together. To ensure chicken production, it is essential to monitor the chickens. Typical monitoring indicators include open beak (OB) behavior, spatial dispersion, and movement of chickens. Conventionally, chicken monitoring was achieved in routinely patrol. However, manually monitoring a large flock of chickens is time-consuming and may not detect adverse events in real-time. Thus, this study proposes to monitor OB behavior, spatial dispersion, and movement of chickens on commercial farms using machine vision. The proposed early warning system comprised customized embedded systems, Wi-Fi mesh, an open-beaked behavior detection model (OBDM), and a chicken detection and tracking model (CDTM). The customized embedded systems comprised single board computers and cameras installed on pillars and roof beams to acquire side-view and top-view videos, respectively, of chickens. The acquired videos were transmitted to a cloud server through Wi-Fi mesh and 4G network. Subsequently, OBDM detected chicken heads in the side-view videos and quantified the ratio of the chickens with OB behaviors (also referred to as OB ratio). CDTM localized chickens in the top-view videos, tracked the chickens and quantified spatial dispersion and movement of the chickens using nearest neighbor (NN) and Bytetrack algorithm, respectively. The safe zones of OB ratio, dispersion, and movement, respectively, were determined using mean and standard deviation, 95% confidence intervals of autoregressive integrated moving average (ARIMA), and 95% confidence intervals seasonal autoregressive integrated moving average with exogenous factors (SARIMAX). The values outside the safe zones were considered as warnings. OBDM achieved an overall mAP of 91.3% in chicken head

detection. CDTM achieved a mAP of 95.8% in chicken localization. CDTM achieved an overall MOTA of 89.5% in chicken tracking. The ARIMA and SARIMAX models, respectively, achieved a mean absolute percentage error (MAPE) of 3.44% and 13.76%. This research can provide an assistance for chicken farmers to more efficiently manage their farms.

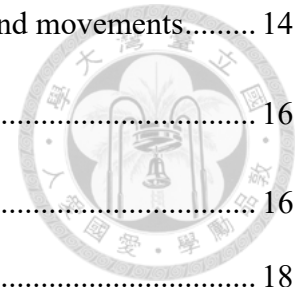
Keywords. Embedded system, nearest neighbor (NN) algorithm, Bytetrack algorithm, deep learning.

TABLE OF CONTENTS



ACKNOWLEDGEMENTS.....	I
摘要	II
ABSTRACT	III
TABLE OF CONTENTS	V
LIST OF FIGURES.....	VII
LIST OF TABLES	X
CHAPTER 1 INTRODUCTION	1
1.1 Background of the study.....	1
1.2 Objectives	2
1.3 Organization	2
CHAPTER 2 LITERATURE REVIEW.....	3
2.1 Traditional approaches for chicken monitor.....	3
2.2 Image processing-based approaches for chicken monitor.....	3
2.3 Deep learning-based approaches for chicken localization and tracking.....	4
CHAPTER 3 MATERIALS AND METHODS.....	6
3.1 Overview of the system	6
3.2 Experimental site	7
3.3 Embedded system	7
3.4 Image collection and annotation.....	9
3.5 OB behavior detection and quantification	11
3.6 Chicken detection and spatial dispersion and movement quantification.....	12

3.7	Monitoring of chicken OB behavior, spatial dispersion, and movements.....	14
CHAPTER 4	RESULTS AND DISCUSSION	16
4.1	Performance of the OB behavior detection	16
4.2	Analysis of chicken OB ratio.....	18
4.3	Performance of the chicken detection and tracking.....	20
4.4	Analysis of chicken spatial dispersion and movement.....	22
4.5	Monitoring and warning of chicken OB behavior, spatial dispersion, and movement	25
CHAPTER 5	CONCLUSION	34
REFERENCE.....		35



LIST OF FIGURES

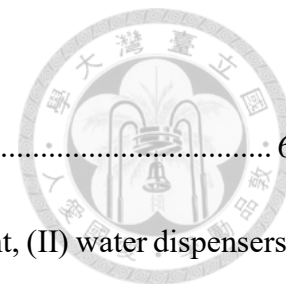
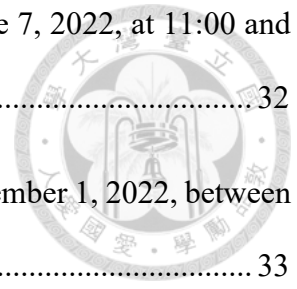


Figure 3.1 Flowchart of the proposed system.....	6
Figure 3.2 Configuration of the chicken house: (I) feeding equipment, (II) water dispensers, and (III) transparent glass.	7
Figure 3.3 (a) The positions of the embedded systems in the chicken house. The side-view and top-view embedded systems were installed on (b) pillars and (c) beams, respectively.	9
Figure 3.4 Collected (a) side-view and top-view images and the annotations.	10
Figure 3.5 Chicken heads with (a) OB and (b) non-OB behaviors.	10
Figure 4.1 (a) Precision-recall curves and (b) confusion matrix of the open-beaked behavior detection model.....	16
Figure 4.2 The challenging scenarios of open-beaked behavior detection: (a) and (b) chickens of various ages, (c) and (d) insufficient illumination, (e) and (f) occlusion, and (g) and (h) rear-facing chicken. Yellow, pink, and purple BBs indicate GT, OB behavior, and non-OB behavior, respectively.	17
Figure 4.3 Mean daily OB ratios and temperatures of the first and second batches acquired by SV ₁ and SV ₂ : (a) and (b) the first and second batches of SV ₁ and (c) and (d) the first and second batches of SV ₂	19
Figure 4.4 Hourly OB ratios and temperatures of the first and second batches acquired by SV ₁ and SV ₂ : (a) and (b) the first and second batches of SV ₁ and (c) and (d) the first and second batches of SV ₂	20
Figure 4.5 Precision-recall curve of the chicken localization in CDTM.....	21

Figure 4.6 The challenging scenarios of chicken localization: (a) and (b) chickens of various ages, (c) overexposure, (d) insufficient illumination, (e) and (f) overlapping, and (g) and (h) occlusion. Yellow and purple BBs indicate GT and chicken, respectively.....	22
Figure 4.7 Mean hourly dispersion values of the first and second batches acquired by TV ₁ , TV ₂ , TV ₃ , and TV ₄ : (a)-(d) the first batch of TV ₁ , TV ₂ , TV ₃ , and TV ₄ and (e)-(h) the second batch of TV ₁ , TV ₂ , TV ₃ , and TV ₄	23
Figure 4.8 Mean hourly movement values of the first and second batches acquired by TV ₁ , TV ₂ , TV ₃ , and TV ₄ : (a)-(d) the first batch of TV ₁ , TV ₂ , TV ₃ , and TV ₄ and (e)-(h) the second batch of TV ₁ , TV ₂ , TV ₃ , and TV ₄	24
Figure 4.9 Hourly movement values and temperatures of the first and second batches acquired by TV ₁ , TV ₂ , TV ₃ , and TV ₄ : (a)-(d) the first batch of TV ₁ , TV ₂ , TV ₃ , and TV ₄ and (e)-(h) the second batch of TV ₁ , TV ₂ , TV ₃ , and TV ₄	25
Figure 4.10 OB behavior in (a) Region 1 and (b) Region 2. The Roman numerals indicate cases to be discussed.....	26
Figure 4.11 Chicken dispersion in (a) Region 1 and (b) Region 2. The Roman numerals indicate cases to be discussed.	27
Figure 4.12 Chicken movement in (a) Region 1 and (b) Region 2. The Roman numerals indicate cases to be discussed.	29
Figure 4.13 The top-view and side-view images in event (I) occurred on June 20, 2022, between 16:30 and 17:30.	30
Figure 4.14 The top-view and side-view images in event (II) occurred on October 9, 2022, between 6:30 and 7:00.	31

Figure 4.15 The top-view images in event (III) occurred on (a) June 7, 2022, at 11:00 and
(b) at 16:00.....32

Figure 4.16 The top-view images in event (IV) occurred on (a) November 1, 2022, between
6:30 and 10:30. 33



LIST OF TABLES

Table 3.1 Amount of training and test images and annotated bounding boxes (BBs).	10
Table 4.1 ROC of the OBDM.....	16
Table 4.2 Evaluation result of chicken tracking in CDTM.	22



CHAPTER 1 INTRODUCTION



1.1 Background of the study

Chicken is a major source of dietary protein worldwide. In 2021, approximately 122 million metric tons of poultry meat were produced worldwide, generating a revenue of \$21.2 billion US dollars (Food and Agriculture Organization, 2022). In Taiwan, around 680 thousand metric tons of chicken products were produced in 2021, accounting for 27.63% of the total animal husbandry sales of the year (Council of Agriculture, Executive Yuan, Taiwan, 2021). Among the chickens, Taiwanese native chickens (TNC) are popular varieties in the domestic market, accounting for 28.48% of the chicken meat market in 2022. These varieties are compared with broiler. Although there exist several recurring problems that impact chicken farming, such as disease outbreaks (Bureau of Animal and Plant Health Inspection and Quarantine, Executive Yuan, Taiwan, 2023) and fluctuation of feed costs (National Animal Industry Foundation, Taiwan, 2021), the TNC industry has continued to grow and expand at a steady pace.

Daily patrol is a routine in the management of TNCs in conventional chicken farming. TNCs are typically raised using floor-rearing approach with intensive densities and have a growth period of 12 to 13 weeks. Because of the long growth period, chicken farmers must invest significant efforts in maintaining chicken health and environmental comfortability to prevent loss. Maintaining a comfortable temperature and odor-free litter is the key to keep the health of TNCs. In the daily patrol, three key indices of chickens are observed: open beak (OB) behavior, spatial dispersion, and movement. The OB behavior can serve as an essential indicator of heat stress, as chickens tend to open beaks and pant when overheated. The spatial dispersion can provide important insights about the environmental

conditions or stress, as chickens often cluster together in stressful situations or poor environmental conditions. The movement can be a reliable indicator of overall health and wellbeing, with changes in movement patterns potentially suggesting a range of issues, from environmental discomfort to illness or injury. Conventional patrols in farms to monitor a large flock of chickens are, however, time-consuming and laborious. Thus, this study proposes to monitor OB behavior, spatial dispersion, and movement of chickens on a commercial chicken farm using machine vision.

1.2 Objectives

This proposed monitoring system comprised three components: 1) customized embedded imaging system to acquire videos of TNCs from side view and top view, 2) two convolutional neural networks (CNNs) to detect chicken mouths and chickens from the side-view and top-view videos, respectively, and 3) a warning model that detect anomalous OB behavior, spatial dispersion, and movement. This monitoring warning system enhances the ability of chicken farmers to detect potential health risks and environmental hazards in chickens.

1.3 Organization

The remaining of this document is organized as follows. In Chapter 2, research of traditional approaches, research of image processing-based approaches, and research of deep learning-based approaches in chicken monitoring are review. In Chapter 3, the collection of videos is presented first. The chicken detection and quantification algorithms are then presented. Last, the warning models are presented. The results of this research are presented in Chapter 4. The conclusions of this study are given in Chapter 5.

CHAPTER 2 LITERATURE REVIEW



2.1 Traditional approaches for chicken monitor

Conventionally, chicken monitoring was evaluated using manual observation and environmental sensors. Lott et al. (1998) measured and controlled air velocities to enhance the weight gain of broilers. Purswell et al. (2012) determined the threshold of heat stress in chickens by using a temperature and humidity sensor. However, previous studies relied on indirect indicators that were unable to accurately represent the subjective experiences of chickens. Therefore, the behavioral characteristics of chickens were considered as more reliable indices.

2.2 Image processing-based approaches for chicken monitor

Applying image processing-based methods provides an effective and efficient approach for monitoring chicken. The implementation of image processing-based monitoring system enables continuous and non-intrusive monitoring of chicken. Several studies have successfully employed image processing methods to for this purpose. Aydin et al. (2010) analyzed different gait score groups to measure the chicken activities from top-view images by calculating the difference of the pixel values between with the previous image. Pereira et al. (2013) identified the behavior of white broiler hens from top-view images by applying a combination of image processing and classification tree, which achieved an accuracy of 70%. Kashiha et al. (2013) developed an animal distribution index to identify abrupt declines in the broiler distribution from top-view images by applying a linear real-time prediction model, which achieved an accuracy of 95.2%. Zhuang et al. (2018) skeletonized a chicken by applying K-means clustering and thinning method. Subsequently, the SVM algorithm was used to recognize the healthy or sick chicken's head and achieved an

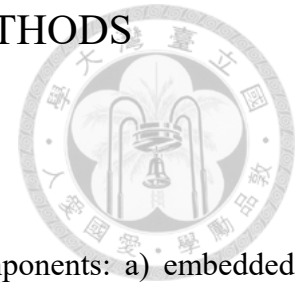
accuracy of 99.5%. However, many of these studies were conducted in controlled experimental settings that exhibited limitations in generalizability and may only work well under specific conditions. Considering that most commercial chicken farms are naturally illuminated and have complex backgrounds in Taiwan, it is necessary to apply a more optimal and objective approach.

2.3 Deep learning-based approaches for chicken localization and tracking

In recent years, convolutional neural networks (CNNs), a method within deep learning model, have emerged as an effective solution for addressing sophisticated tasks in machine vision. The CNN model comprises millions of neurons to learn the key features from input images. Zhuang and Zhang (2019) identified sick broilers within a flock by applying a CNN of an improved feature fusion single-shot multibox detector architecture. Guo et al. (2022) detected chicken behaviors (i.e., feeding, drinking, standing, and resting) at different ages by applying a CNN of DenseNet-264 network architecture. Yu et al. (2022) detected poultry heat stress state (i.e., wing droop, wing spread, and open mouth panting) by applying a CNN of the improved FPN-DenseNet-SOLO model. Zhu et al. (2022) proposed a method to count chickens by applying a CNN of you only look once version 5x (YOLO v5x; Jiang et al., 2022) architecture. Furthermore, certain studies have successfully combined CNN models with tracking algorithms to provide an efficient monitoring system for chicken farmers. Lin et al. (2020) localized chickens by applying a CNN of Faster R-CNN model and tracked the detected chickens by applying a simple online and real-time tracking algorithm (SORT; Bewley et al., 2016). Sun et al. (2019) improved the tracking of aggregation behavior in broilers by using a CNN of You Only Look Once—version 3 and tracking algorithms of Kalman filter (Kalman, 1960) and Hungarian algorithm (Kuhn, 1955). Siriani et al. (2022) successfully detected and tracked chickens to calculate chicken

movement in low-resolution videos by applying a CNN of the modified YOLO v4 architecture (Bochkovskiy et al., 2020) and a Kalman filter. Neethirajan (2022) improved the process of tracking chickens by applying a CNN of YOLO v5 and a deep SORT (Wojke et al., 2017). The aforementioned studies provide evidence that tracking-by-detection strategies can effectively and precisely perform in numerous applications.

CHAPTER 3 MATERIALS AND METHODS



3.1 Overview of the system

The system for monitoring chicken was composed of three components: a) embedded systems, b) two deep learning models (open-beaked behavior detection model, OBDM; chicken detection and tracking model, CDTM), and c) warning models (Configuration of the chicken house: (I) feeding equipment, (II) water dispensers, and (III) transparent glass. Figure 3.1). The embedded systems recorded side-view and top-view videos of chickens and collected the temperature in chicken farms. The OBDM detected chicken heads in the side-view videos and quantified the ratio of the chickens with OB behaviors (also referred to as OB ratio). The CDTM localized and tracked chickens in the top-view videos and, subsequently, quantified the spatial dispersion and movement of the chickens. The warning model determined the safe zones of the OB ratio, spatial dispersion, and movement of the chickens (Figure 3.1d).

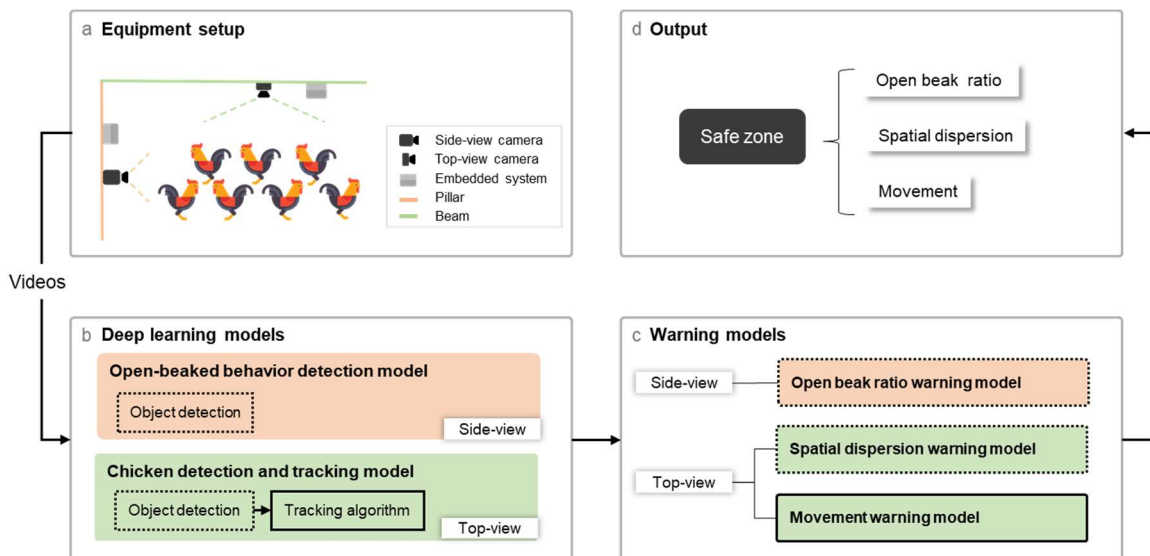


Figure 3.1 Flowchart of the proposed system.

3.2 Experimental site

The experiment was conducted at Hsin-Ho chicken house (Leadray Livestock Co., Ltd; Huwei, Yunlin, Taiwan; Figure 3.2). The house was approximately 113×14.8 m and was equipped with feeding buckets (I in Figure 3.2) and water dispensers (II in Figure 3.2). The house was naturally illuminated using transparent glasses in the side wall (III in Figure 3.2), making the illumination conditions vary considerably. Approximately twenty thousand red-feathered TNCs were raised in the house. In this study, the term "chicken" specifically refers to red-feathered TNC, which is a popular variety in Taiwan. A Wi-Fi mesh network was developed in the house to provide seamless Wi-Fi coverage throughout the house.

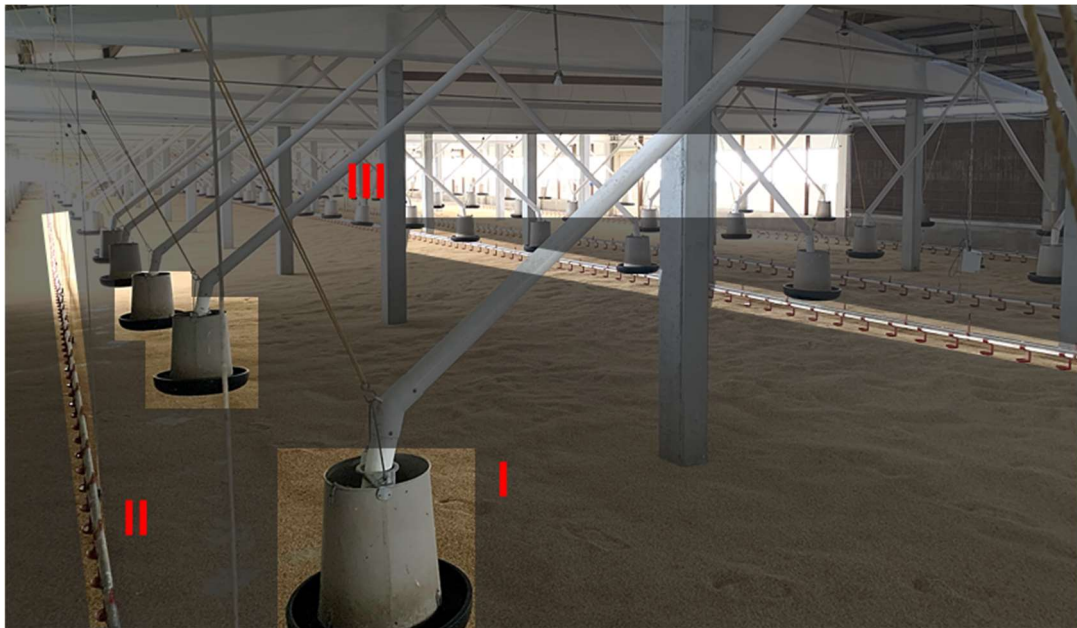
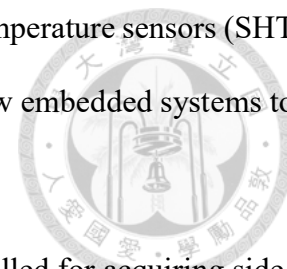


Figure 3.2 Configuration of the chicken house: (I) feeding equipment, (II) water dispensers, and (III) transparent glass.

3.3 Embedded system

Each embedded system was composed of a single board computer (Raspberry Pi 3 Model B+, Raspberry Pi Foundation; Cambridge, UK), a camera, and a watertight box. Webcams (HD Pro C920, Logitech; Lausanne, Switzerland) were used as the cameras for acquiring side-view videos. Wide-angle distortion-free USB cameras (KS2A17, Kingsen; Shenzhen,

China) were used as the cameras for acquiring top-view videos. Temperature sensors (SHT 31, Sensirion; Stäfa, Switzerland) were integrated into the side-view embedded systems to collect temperature data.



A total of two and four embedded systems, respectively, were installed for acquiring side-view and top-view videos from two regions in the chicken house (Figure 3.3a). The side-view embedded systems (SV₁ and SV₂) were installed on pillars in the chicken house and were approximately 0.4 m above the ground (Figure 3.3b). The top-view embedded systems (TV₁, TV₂, TV₃, and TV₄) were installed on beams of the chicken house and were approximately 3.0 m above the ground (Figure 3.3c). The side-view and top-view embedded systems were deployed in two regions, denoted as Region 1 and Region 2 for the purpose of video acquisition. Videos were acquired at a resolution of 1920 × 1080 and 1280 × 1024 pixels, respectively, for the side-view and top-view videos. Each video was acquired at 5 frames per second (fps) and was 5-minute long. The temperature of the chicken house was measured every minute. The videos and environmental information were uploaded to a cloud storage through the Wi-Fi mesh network.

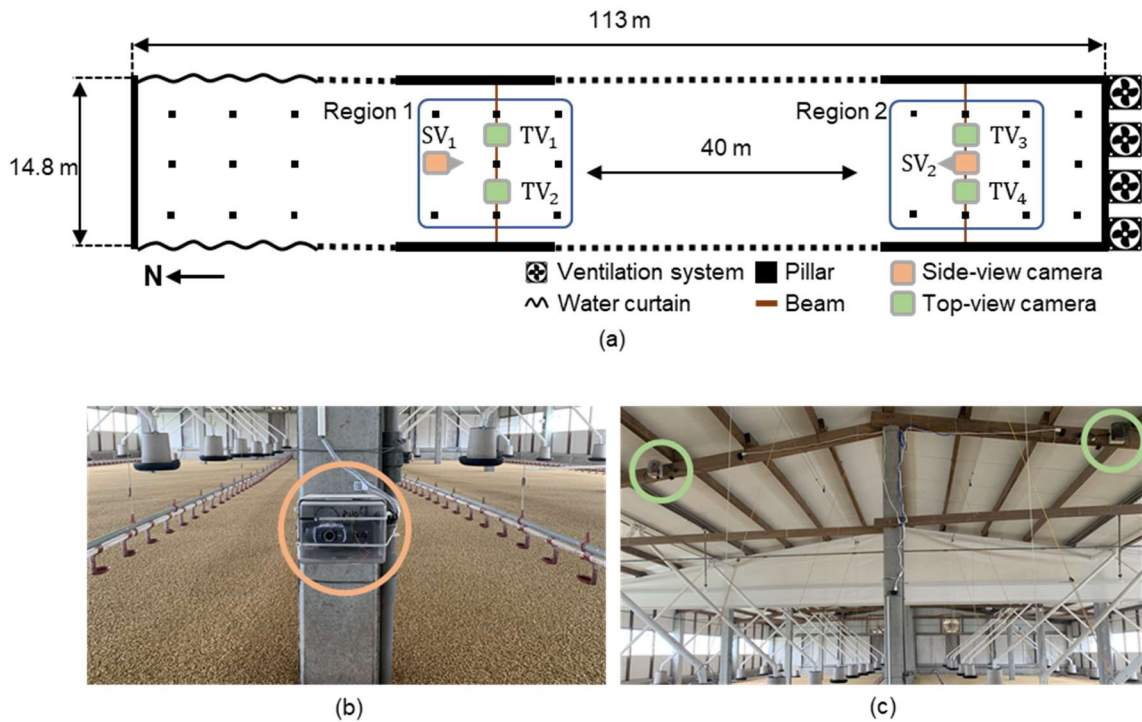


Figure 3.3 (a) The positions of the embedded systems in the chicken house. The side-view and top-view embedded systems were installed on (b) pillars and (c) beams, respectively.

3.4 Image collection and annotation

The side-view and top-view videos were collected between May and November, 2022. During the period, two batches of chickens were raised. The chickens were brought into the house when they were 4-week old and were sent for slaughter when they were 10-week old. The first batch was raised between May and July, whereas the second batch was raised between September and November. The videos of the chickens were collected continuously between 06:00 and 18:00. More than 1,400 hours of side-view and top-view videos were collected. Certain videos were missing due to network instability. A thousand images were randomly converted from the side-view and top-view videos, respectively, for model training and test (Figure 3.4).



Figure 3.4 Collected (a) side-view and top-view images and the annotations.

For the side-view images, chicken heads larger than 40 pixels were annotated. The annotated chicken heads were categorized into OB and non-OB behaviors. A chicken with a beak-tip open greater than 10 pixels were defined as an OB (Figure 3.5a); otherwise, it was classified as non-OB (Figure 3.5b). For the top-view images, chickens were annotated (Figure 3.4b). The annotation was performed using LabelImg (Heartex, 2015). The annotated images were split into training and test dataset at a ratio of 4:1 (Table 3.1).

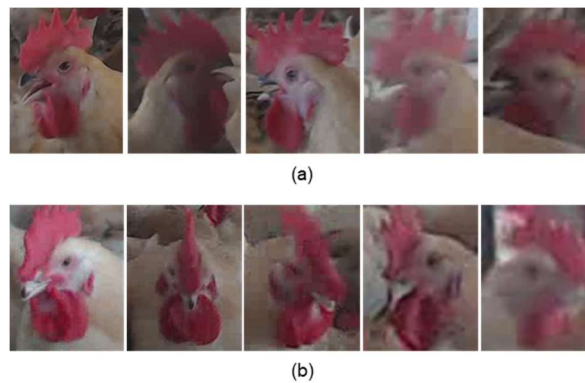


Figure 3.5 Chicken heads with (a) OB and (b) non-OB behaviors.

Table 3.1 Amount of training and test images and annotated bounding boxes (BBs).

Perspective	Category	Images		BBs	
		Training	Test	Training	Test
Side view	OB	800	200	4,475	1,465
	Non-OB			5,687	2,388
Top view	Chicken	800	200	113,161	30,888

3.5 OB behavior detection and quantification

You Only Look Once—version 7 tiny (YOLO v7-tiny; Wang et al., 2022) was used as the architecture for OBDM to detect chickens with OB and non-OB behaviors in the side-view images. To train the model, the dimension of the input images to OBDM was set to 640×640 pixels. Online image augmentations were next implemented to enhance model robustness during training. The augmentation operations included hue, saturation, brightness, horizontal flipping, mosaic and mix-up. Stochastic gradient descent (SGD; Bottou, 2012) was used as the optimizer.

The hyperparameters of the OBDM, including image augmentations, SGD, and learning rate, were selected using genetic algorithm (Mirjalili & Mirjalili, 2019). Five initial population, containing five sets of the hyperparameters as chromosomes, iterated 300 generations with a mutation probability of 0.8. A fitness function was used to evaluate the hyperparameters during the mutation and evolutionary process. The fitness function was defined as a weighted combination of mean average precision (mAP) at an intersection-over-union (IoU) threshold of 0.5 ($\text{mAP}@0.5$) and mAP at IoU thresholds between 0.5 and 0.95 ($\text{mAP}@0.5:0.95$). The weights of $\text{mAP}@0.5$ and $\text{mAP}@0.5:0.95$ were 0.2 and 0.8, respectively. According to the optimized hyperparameters, the hue, saturation, and brightness were applied to each training image by multiplying a uniform random value between 1 ± 0.015 , 1 ± 0.71 , and 1 ± 0.458 , respectively. The horizontal flipping, mosaic, and mix-up were applied to the images with a probability of 0.415, 0.8 and 0.0362, respectively. The momentum and weight decay of SGD were configured as 0.98 and 0.0058, respectively. The model was trained for 300 epochs with a batch size of 32. The learning rate was warmed up to 0.00758 in 2.4 epochs and decreased to 0.0000758 at the end of the model

training. A GPU (TITAN RTX, NVIDIA; Santa Clara, USA) was used for training the model.

After the model training, the OB behaviors was computed as the ratio of chickens with OB behavior to the total number of chickens in the images (i.e., OB ratio). Each OB ratio was evaluated for a video of 5-minute length (i.e., 1500 frames).

3.6 Chicken detection and spatial dispersion and movement quantification

The CDTM was composed of a convolutional neural network for chicken localization, nearest neighbor (NN; Clark & Evans, 1954) algorithm for calculating the spatial dispersion of chickens, and Bytetrack algorithm (Zhang et al., 2022) for calculating chicken movements. YOLO v7-tiny was again used to localize chickens in CDTM. The dimension of the input images to the CDTM was set to 416×416 pixels before the model training. The online augmentation operations, including hue, saturation, brightness, horizontal flipping, mosaic and mix-up, enhanced model robustness. SGD was used as the optimizer. The hyperparameters of the CDTM, including image augmentations. SGD, and learning rate, were selected using genetic algorithm. Five initial population, containing five sets of the hyperparameters as chromosomes, iterated 300 generations with a mutation probability of 0.8. The fitness function was used the same as the OBDM. According to the optimized hyperparameters, the hue, saturation, and brightness were applied to each training image by multiplying a uniform random value between 1 ± 0.015 , 1 ± 0.7 , and 1 ± 0.4 , respectively. The horizontal flipping, mosaic and mix-up were applied to the images with a probability of 0.5, 1 and 0.05, respectively. The momentum and weight decay of SGD were configured as 0.937 and 0.0005, respectively. The model was trained for 300 epochs with a batch size of 16. The learning rate was warmed up to 0.001 in 3 epochs and decreased to 0.00001 at

the end of the model training. A GPU (TITAN RTX, NVIDIA; Santa Clara, USA) was used for training the model.

The spatial dispersion of the chickens in an image was quantified using the centroids of the chickens detected by the YOLO v7-tiny and NN algorithm in CDTM. Spatial dispersion was calculated as:

$$\text{Dispersion} = \frac{\overline{D}_O}{\overline{D}_E}, \quad (1)$$

where \overline{D}_O is the average distance between each chicken and its nearest neighbor in the image and \overline{D}_E is the expected average distance between each chicken and its nearest neighbor. A dispersion value indicated the densely populated chickens, whereas a low dispersion value indicated the sparsely populated chickens. The spatial dispersion of a 5-minute video was calculated as the average of the dispersion values computed for each of the 1500 frames in the video, yielding a total of 110 dispersion values daily.

The movement of the chickens was quantified using the centroids of the chickens detected by the YOLO v7-tiny in CDTM in consecutive frames (i.e., 1500 frames in a 5-minute video) and Bytetrack algorithm. The Bytetrack algorithm was employed to track for all detected BBs in order to improve tracking performance instead of solely focusing on high confidence score BBs. The Bytetrack algorithm predicted the centroids of chicken and BB dimensions by incorporating the information from the previous frame. The BBs (i.e. chicken) detected by the YOLO v7-tiny were separated into high confidence score BBs and low confidence score BBs (e.g. occluded chickens), with a confidence threshold of 0.6. Initially, the high confidence score BBs were used to track the chicken with an IoU between consecutive frames higher than 0.5. When the IoU was lower than 0.5, the low confidence score BBs were used to track the chicken in consecutive frames. If the tracked BBs

remained unmatched for 50 frames, its centroid coordinates were removed. The Euclidean distance between the coordinates of the center of the successfully tracked chickens in consecutive frames was used to calculate the movement of each chicken. A movement value was yielded for each video of 5-minute length (i.e., 1500 frames), yielding a total of 110 movement values daily.

3.7 Monitoring of chicken OB behavior, spatial dispersion, and movements

Mean and standard deviation of the OB ratios from the two batches was used to determining the threshold for the OB ratio. A high OB ratio can potentially induce heat stress. Thus, monitoring of the OB ratio was primarily oriented towards OB ratios exceeding the determined threshold. The threshold was established based on two standard deviations. The OB ratios below the threshold were defined as the normal. The OB ratios exceeding the threshold were defined as the preliminary warnings (yellow). If the preliminary warnings persisted for an hour, the OB ratios were upgraded to critical warnings (red).

An autoregressive integrated moving average (ARIMA; Box et al., 2015) model was used to predict chicken dispersion and the safe zone of the dispersion. The dispersion values exhibited a positive correlation with the chicken growth (Figure 4.7). Thus, the dispersion was regarded as a time-series data. The ARIMA model predicted the mean dispersion values of a day using the daily mean dispersion values from past days. An ARIMA model includes three parameters: autoregressive (AR), integrated (I), and moving average (MA). The degree of I was set to 1, since the dispersion values were non-stationary. The order of AR and MA were set to 3 and 4, respectively, using Akaike information criterion. The ARIMA model also predicted the 95% confidence interval of the mean daily dispersion value. In this study, the 95% confidence interval of the dispersion value was marked as the safe zone. The dispersion values outside the 95% confidence interval were marked as

preliminary warnings (yellow). If the preliminary warnings persisted for an hour, the dispersion values were upgraded to critical warnings (red).

A seasonal autoregressive integrated moving average with exogenous factors (SARIMA; Box et al., 2015) model was used to predict chicken movement and the safe zone of the movement. The movement exhibited a seasonal pattern by hour (Figure 4.9). Thus, the movement was regarded as a seasonal time-series data. The SARIMAX model predicted the mean hourly movement values of a day using the hourly mean movement values from past days. An SARIMAX model includes seven parameters: AR, I, MA, seasonal AR, seasonal I, seasonal MA, and seasonal period. The degree of I and seasonal I were set to 0 and 1, respectively, since the movement values with seasonal patterns were non-stationary. The order of AR, MA, seasonal AR, and seasonal MA were set to 0, 5, 3 and 2, respectively, using Akaike information criterion. The seasonal period was set to 12 because the maximum number of hourly mean movement values was collected from 06:00 to 18:00 each day. Moreover, the hourly mean movement values and temperatures had an opposite trend. As a result, the temperature was considered an external variable to improve the model robustness and accuracy. The SARIMAX model also predicted the 95% confidence interval of the mean hourly movement value. In this study, the 95% confidence interval of the movement value was marked as the safe zone. The movement values outside the 95% confidence interval were marked as preliminary warnings (yellow). If the preliminary warnings persisted for 30 minutes, the movement values were upgraded to critical warnings (red).

CHAPTER 4 RESULTS AND DISCUSSION



4.1 Performance of the OB behavior detection

The detection performance of the OBDM was evaluated using receiver operating characteristic (ROC; Fawcett, 2006) analysis and the 200 side-view test images. In the evaluation, the confidence score threshold for positive detection was set to 0.25. A detection was regarded as a true positive (TP) if the IoU between two BBs predicted by the model and the corresponding ground truth (GT) exceeded 0.65; otherwise, it was regarded as a false positive (FP). A detection was regarded as a false negative (FN) if the predicted BB had no associated GT BB. The OBDM achieved an overall precision of 83.2%, an overall recall of 81.8%, an overall F1 score of 82.5%, and a mean average precision (mAP; Everingham et al., 2010) of 91.3% (Table 4.1) in chicken head detection. The precision-recall curves (Manning & Schutze, 1999) and the confusion matrix of the two classes (OB and non-OB behaviors) were illustrated in Figure 4.1.

Table 4.1 ROC of the OBDM.

Category	Precision (%)	Recall (%)	F1-score (%)	AP (%)
OB	81.8	85.9	83.8	92.4
Non-OB	84.5	77.8	81.1	90.3
Overall	83.2	81.8	82.5	91.3

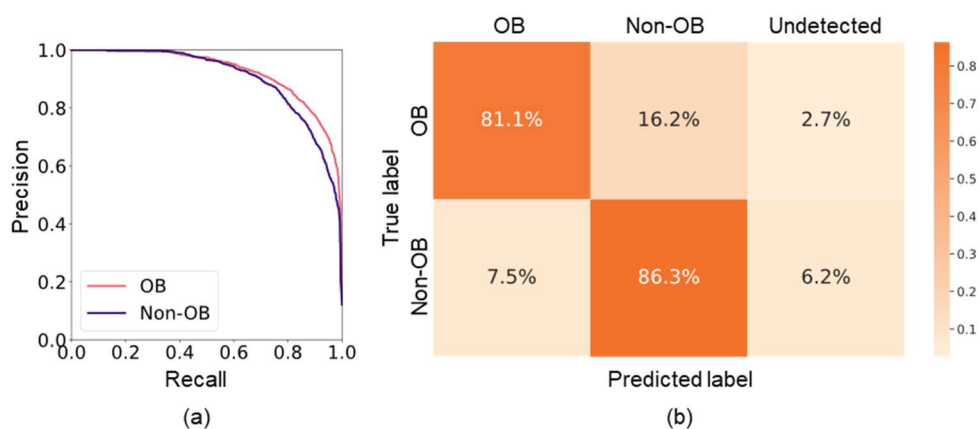


Figure 4.1 (a) Precision-recall curves and (b) confusion matrix of the open-beaked behavior detection model.

To assess the robustness of the trained OBDM, four challenging scenarios were examined: chickens of various ages, insufficient illumination, occlusion, and rear-facing chicken (Figure 4.2). In certain scenarios, images of 5-week-old and 10-week-old (Figure 4.2a and 4.2b) chickens were collected. The chickens exhibited distinct features on their heads. In certain other scenarios, the illuminations of the images were low (Figure 4.2c and 4.2d). Nevertheless, the chickens were successfully detected and accurately classified in these scenarios. However, in certain other scenarios, FP or FN occurred. In certain other scenarios, chickens overlapped each other and the details of the occluded chickens were missing, resulting in FP (Figure 4.2e) or FN (Figure 4.2f) detections. In certain other scenarios, chickens faced away from the camera and the visible details of the chicken mouths were minimal, resulting in FP (Figure 4.2g) or FN (Figure 4.2h) detections.

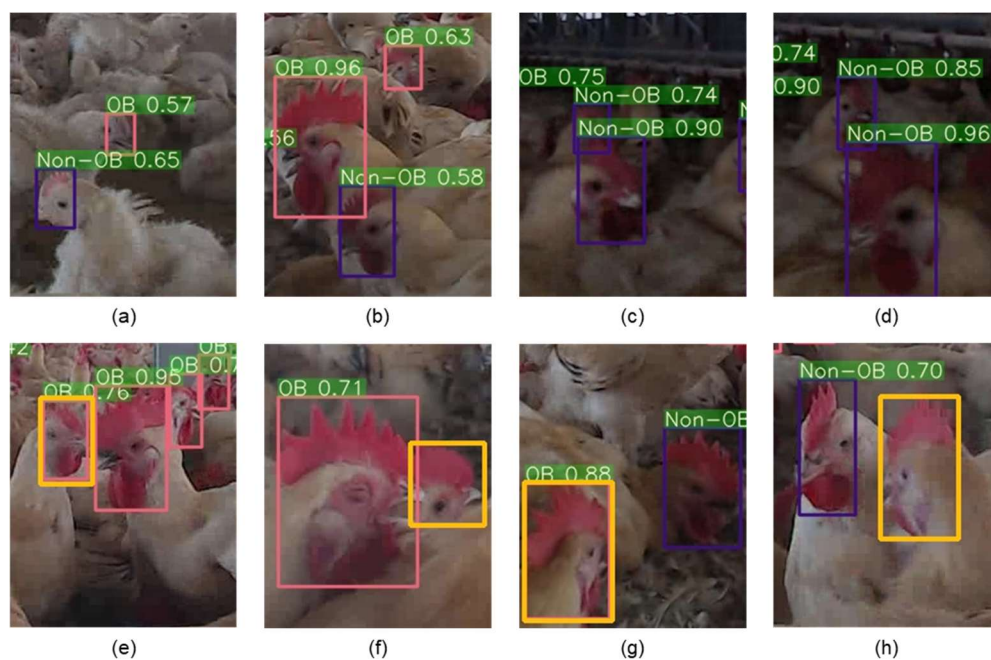
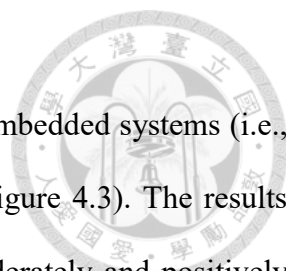


Figure 4.2 The challenging scenarios of open-beaked behavior detection: (a) and (b) chickens of various ages, (c) and (d) insufficient illumination, (e) and (f) occlusion, and (g) and (h) rear-facing chicken. Yellow, pink, and purple BBs indicate GT, OB behavior, and non-OB behavior, respectively.

4.2 Analysis of chicken OB ratio



The mean daily OB ratios and temperatures of the two side-view embedded systems (i.e., SV₁ and SV₂) for the two batches of chickens were illustrated (Figure 4.3). The results indicated that the mean daily OB ratio and temperature were moderately and positively correlated ($r_{SV1} = 0.495$, $r_{SV2} = 0.589$). For the videos acquired by SV₁, the OB ratios between weeks 7 and 9 of the first batch were significantly higher than those of the second batch (Figure 4.3a and 4.3b; t-test: $t = 7.384$, $p < 0.001$). The mean temperatures between weeks 7 and 9 of the first and second batch were 33.2°C and 28.3°C, respectively. Similarly, for the videos acquired by SV₂, the mean OB ratios between weeks 7 and 9 of the first batch were significantly higher than those of the second batch (Figure 4.3c and 4.3d; t-test: $t = 3.597$, $p < 0.001$). The mean temperatures between weeks 7 and 9 of the first and second batch were 32.5°C and 28.2°C, respectively. These observations indicate that the chickens are sensitive to high temperatures and tend to exhibit higher OB ratios at higher temperatures.

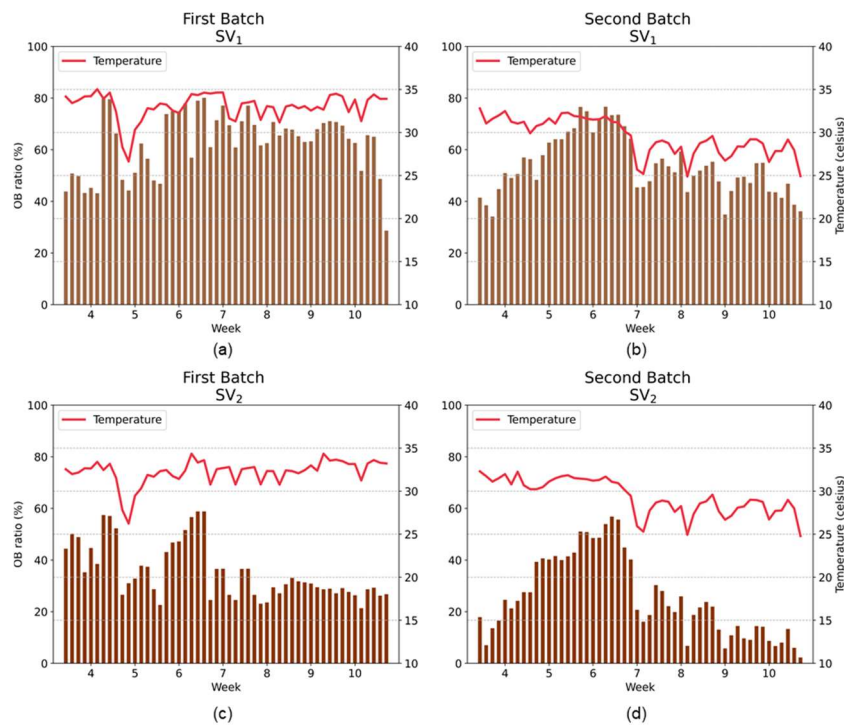


Figure 4.3 Mean daily OB ratios and temperatures of the first and second batches acquired by SV_1 and SV_2 : (a) and (b) the first and second batches of SV_1 and (c) and (d) the first and second batches of SV_2 .

The hourly OB ratios and temperatures between 06:00 and 18:00 of the two batches were illustrated (Figure 4.4). The OB ratios and temperatures had a similar trend ($r_{SV1} = 0.952$, $r_{SV2} = 0.956$). Both the OB ratios and temperatures were low in the morning and evening and peaked around 14:00. Scheffé's multiple comparison tests (Lee & Lee, 2018) indicated that the mean OB ratios between 12:00 and 14:00 were significantly higher than those between 6:00 and 9:00 (ANOVA; $SV_1: F = 38.904, p < 0.001$; $SV_2: F = 40.372, p < 0.001$). This observation indicates that chicken OB ratios are subject to variation in accordance with the prevailing temperatures.

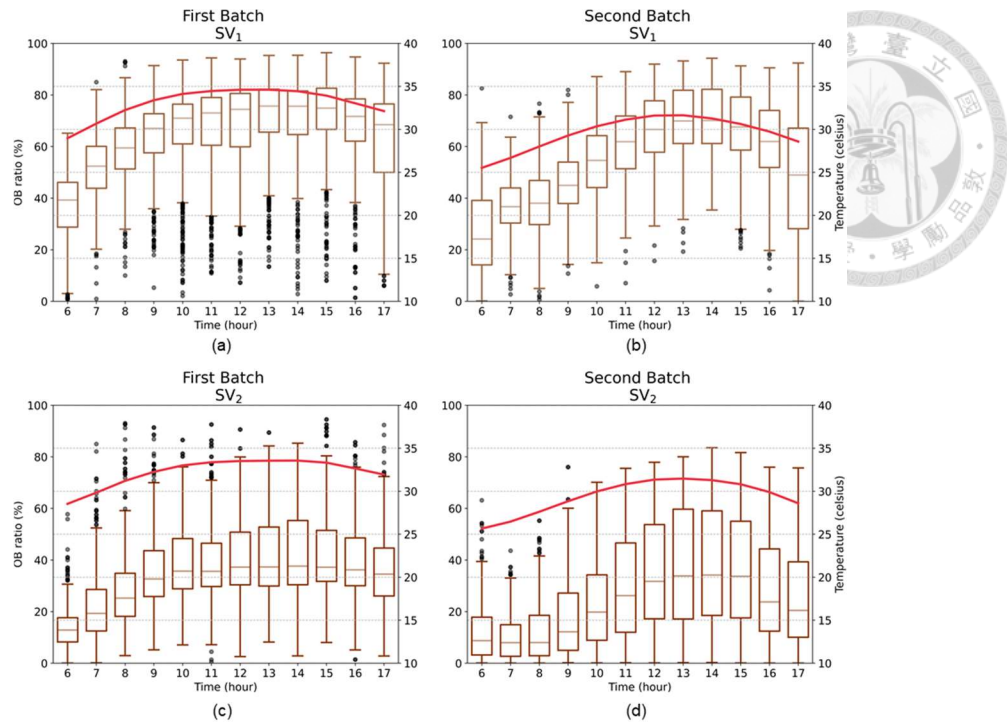


Figure 4.4 Hourly OB ratios and temperatures of the first and second batches acquired by SV_1 and SV_2 : (a) and (b) the first and second batches of SV_1 and (c) and (d) the first and second batches of SV_2 .

4.3 Performance of the chicken detection and tracking

The detection performance of the CDTM was evaluated using ROC analysis and the 200 top-view test images. In the evaluation, the confidence score threshold for positive detection was set to 0.6. The IoU threshold for TP, FP, and FN detection was set to 0.65. The CDTM achieved a precision of 91.1%, a recall of 92.9%, a F1 score of 91.9%, and a mAP of 95.8% in chicken localization. The precision-recall curve of chicken localization was illustrated in Figure 4.5.

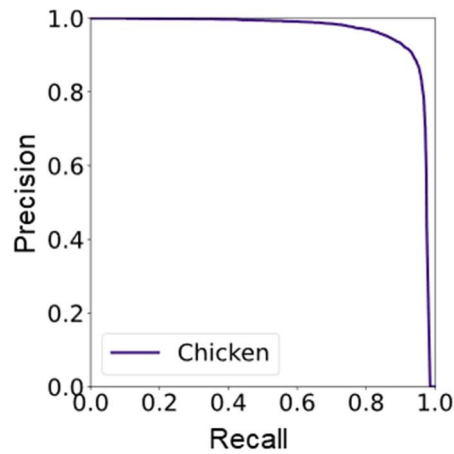


Figure 4.5 Precision-recall curve of the chicken localization in CDTM.

To assess the robustness of the CDTM, five challenging scenarios were examined: chickens of various ages, overexposure, insufficient illumination, overlapping, and occlusion. In certain scenarios, images of 4-week-old and 10-week-old (Figure 4.6a and 4.6b) chickens were acquired. The chickens exhibited distinct features in their appearance. In certain other scenarios, the collected images were overexposed (Figure 4.6c) or with insufficient illumination (Figure 4.6d). Nevertheless, the chickens were successfully detected under these scenarios. However, in certain other scenarios, FN occurred. In certain other scenarios, several chickens overlapped each other (Figure 4.6e and 4.6f), resulting in FN detections. In other certain scenarios, chickens occluded by pipelines, pillars, feeding equipment, or water dispensers in the images (Figure 4.6g and 4.6h), resulting in FN detections.

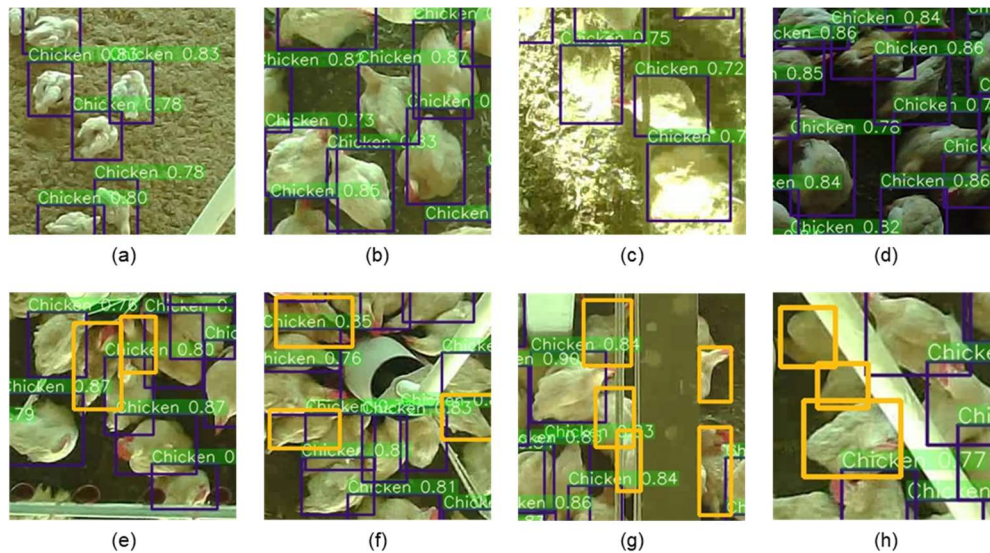


Figure 4.6 The challenging scenarios of chicken localization: (a) and (b) chickens of various ages, (c) overexposure, (d) insufficient illumination, (e) and (f) overlapping, and (g) and (h) occlusion. Yellow and purple BBs indicate GT and chicken, respectively.

The tracking performance of the CDTM was evaluated using multiple object tracking (MOT) metrics (Milan et al., 2016) and two videos of active and stationary chickens. The two videos contained 150 consecutive frames (30 s). The GTs of the chickens were labeled using Dark label (Darkpgmr, 2020). The CDTM approach achieved an overall MOT accuracy (MOTA) of 89.5% in chicken tracking (Table 4.2).

Table 4.2 Evaluation result of chicken tracking in CDTM.

Status	Frame	GT	MT	PT	ML↓	IDs↓	Precision↑	Recall↑	MOTA↑
Active	150	274	237	29	8	15	96.0 %	90.3 %	86.4 %
Stationary	150	116	109	7	0	1	96.8 %	95.7 %	92.5 %
Overall	300	390	346	36	8	16	96.4 %	93.0 %	89.5 %

Frame = number of frame; GT = number of piglets in the crate; MT = number of mostly tracked; PT = number of partially tracked; ML = number of mostly lost; IDs = ID switching; MOTA = multiple object tracking accuracy; ↑/↓ = higher / lower scores denote better performance.

4.4 Analysis of chicken spatial dispersion and movement

The mean hourly dispersion values and their 95% confidence intervals of the four top-view embedded systems (i.e., TV₁, TV₂, TV₃, and TV₄) for the two batches of chickens were illustrated (Figure 4.7). The mean hourly dispersion values increased gradually. For the videos acquired by TV₁, TV₂, TV₃, and TV₄, the correlation coefficients between dispersion and chicken age (in day) were between 0.657 and 0.931. The dimension of the chicken

house is fixed. Thus, the space between the chickens decreased as the chicken grew, contributing to an upward trend in dispersion. Moreover, the chickens exhibited a tendency to migrate towards the air inlet. Region 1 (i.e., TV₁ and TV₂; Figure 3.3a) were closer to the air inlet than Region 2 (i.e., TV₃ and TV₄). Thus, the mean dispersion values of TV₁ and TV₂ were significantly larger than those of TV₃ and TV₄ (ANOVA; First batch: $F = 116.079, p < 0.001$, Second batch: $F = 156.529, p < 0.001$).

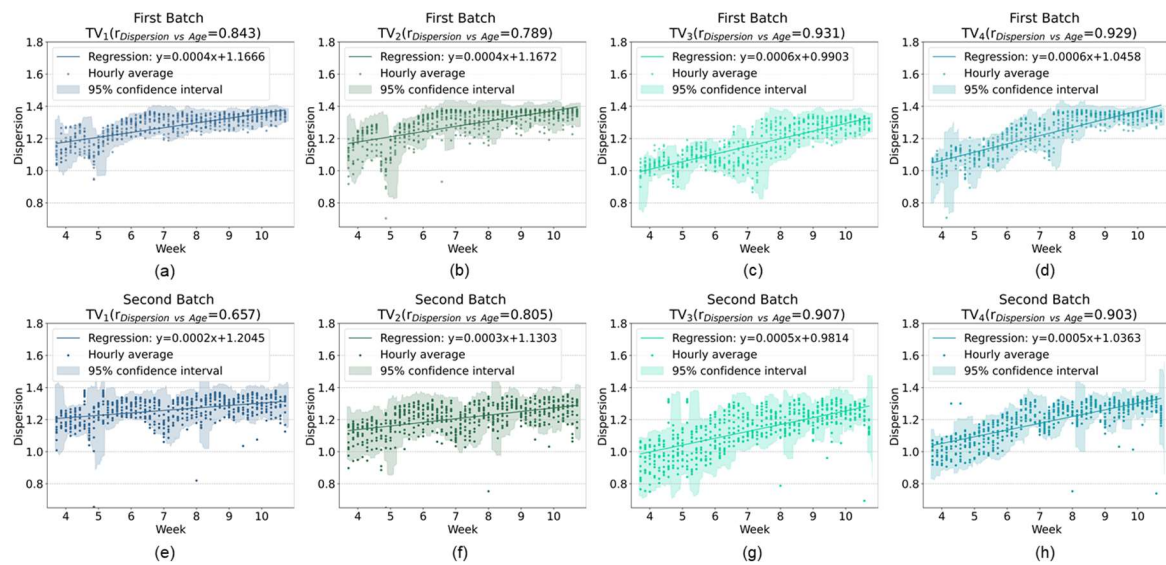


Figure 4.7 Mean hourly dispersion values of the first and second batches acquired by TV₁, TV₂, TV₃, and TV₄: (a)-(d) the first batch of TV₁, TV₂, TV₃, and TV₄ and (e)-(h) the second batch of TV₁, TV₂, TV₃, and TV₄.

The mean hourly movement values and their 95% confidence intervals of the four top-view embedded systems (i.e., TV₁, TV₂, TV₃, and TV₄) for the two batches of chickens were illustrated (Figure 4.8). The results indicate that the movement and temperature were moderately and negatively correlated for the two batches ($r_{TV1} = -0.488$, $r_{TV2} = -0.521$, $r_{TV3} = -0.486$, $r_{TV4} = -0.369$). For the videos acquired by TV₁, TV₂, TV₃, and TV₄, the mean hourly movement values of the first batch showed a decreasing trend (Figure 4.8a-d) because the mean temperatures between weeks 4 and 6 (31.29°C at TV₁ and TV₂; 31.46°C at TV₃ and TV₄) was lower than those between weeks 7 and 10 (33.31°C at TV₁ and TV₂; 32.67°C at TV₃ and TV₄). Conversely, the mean hourly movement values of the second batch showed an increasing trend (Figure 4.8e-h) because the mean temperatures between

weeks 4 and 6 (31.53°C at TV₁ and TV₂; 31.32°C at TV₃ and TV₄) was higher than those between weeks 7 and 10 (28.38°C at TV₁ and TV₂; 28.29°C at TV₃ and TV₄). These observations indicate that the chickens tend to exhibit lower movement values at high temperatures.

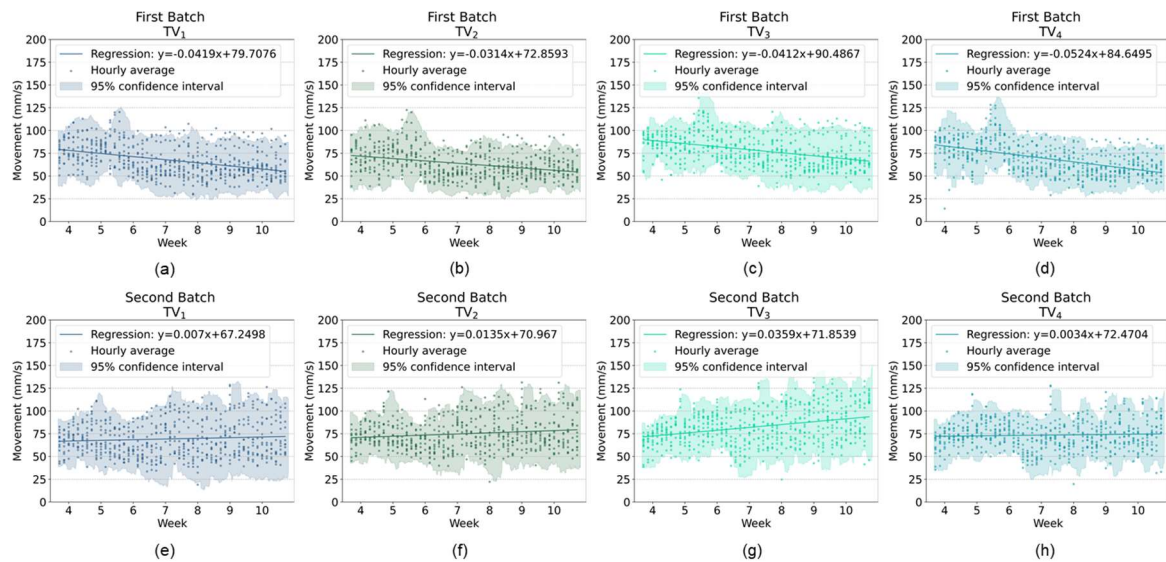


Figure 4.8 Mean hourly movement values of the first and second batches acquired by TV₁, TV₂, TV₃, and TV₄: (a)-(d) the first batch of TV₁, TV₂, TV₃, and TV₄ and (e)-(h) the second batch of TV₁, TV₂, TV₃, and TV₄.

The hourly movement values and temperatures between 06:00 and 18:00 of the two batches were illustrated (Figure 4.9). The movement values and temperatures had an opposite trend ($r_{TV1} = -0.611$, $r_{TV2} = -0.854$, $r_{TV3} = -0.692$, $r_{TV4} = -0.768$). The movement values were high in the morning and evening and bottomed around noon. On the contrary, the temperatures were low in the morning and evening and peaked around noon. Scheffé's multiple comparison tests indicated that the mean movement values between 12:00 and 15:00 were significantly lower than those between 6:00 and 9:00 (ANOVA; TV₁: $F = 109.674$, $p < 0.001$; TV₂: $F = 106.218$, $p < 0.001$; TV₃: $F = 98.828$, $p < 0.001$; TV₄: $F = 72.849$, $p < 0.001$). This observation indicates that chicken movement is influenced by temperature.

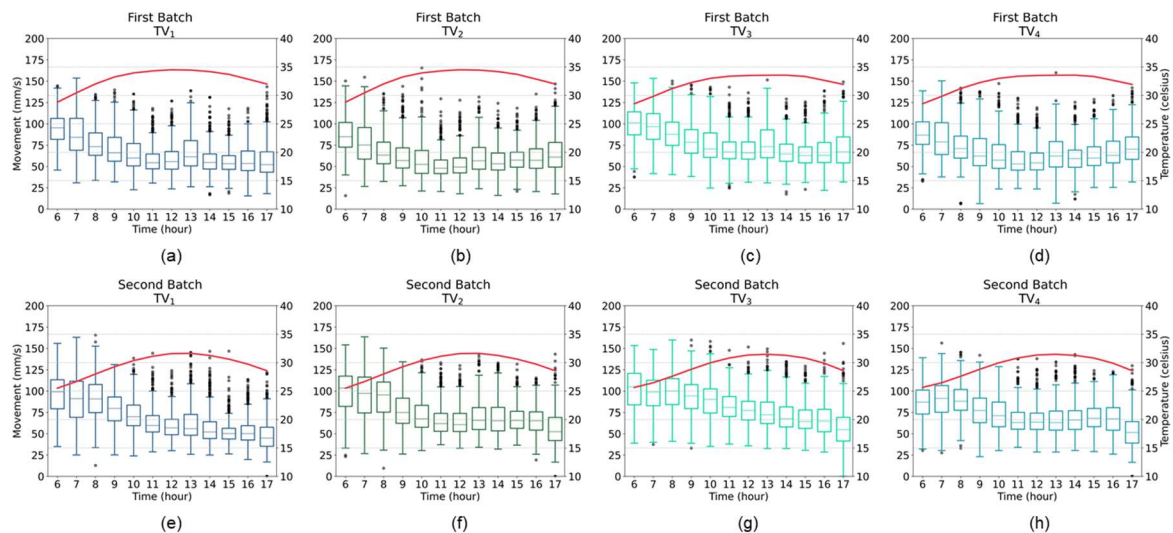


Figure 4.9 Hourly movement values and temperatures of the first and second batches acquired by TV_1 , TV_2 , TV_3 , and TV_4 : (a)-(d) the first batch of TV_1 , TV_2 , TV_3 , and TV_4 and (e)-(h) the second batch of TV_1 , TV_2 , TV_3 , and TV_4 .

4.5 Monitoring and warning of chicken OB behavior, spatial dispersion, and movement

The proposed approach was applied to detect anomalous OB behaviors (Figure 4.10). The overall mean and standard deviation of the OB ratio were 44.32% and 17.96%, respectively. The threshold was set to 80.24% (i.e., mean + 2 standard deviations). In Region 1 (i.e., SV_1), 12 and 11 critical warning events, respectively, occurred in the first and second batches. The critical warning events occurred more frequently when the temperature exceeded 30°C . Conversely, in Region 2 (i.e., SV_2), no critical warning events occurred in either the first or second batches. Despite there was only a mere temperature difference of 1 to 2°C between Regions 1 and 2, this small variation could have a significant impact on the critical warning events, especially when the temperature exceeded 30°C .

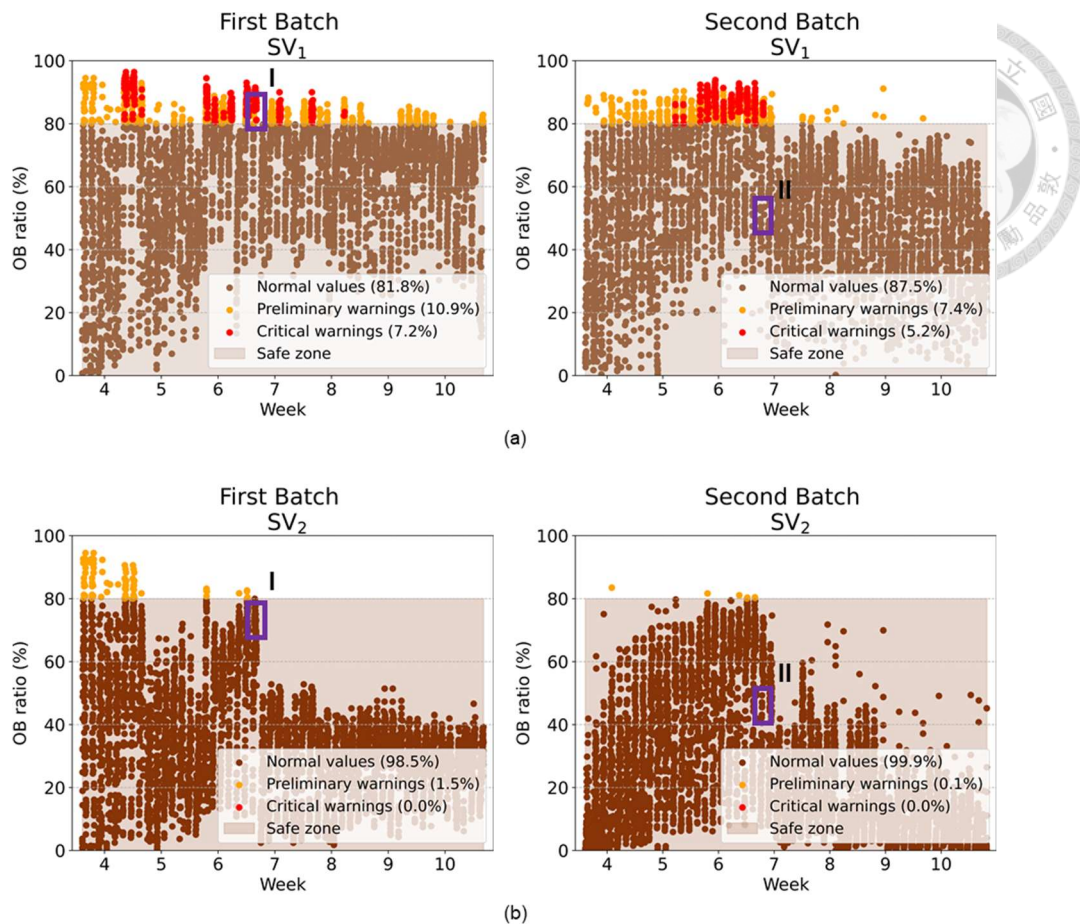
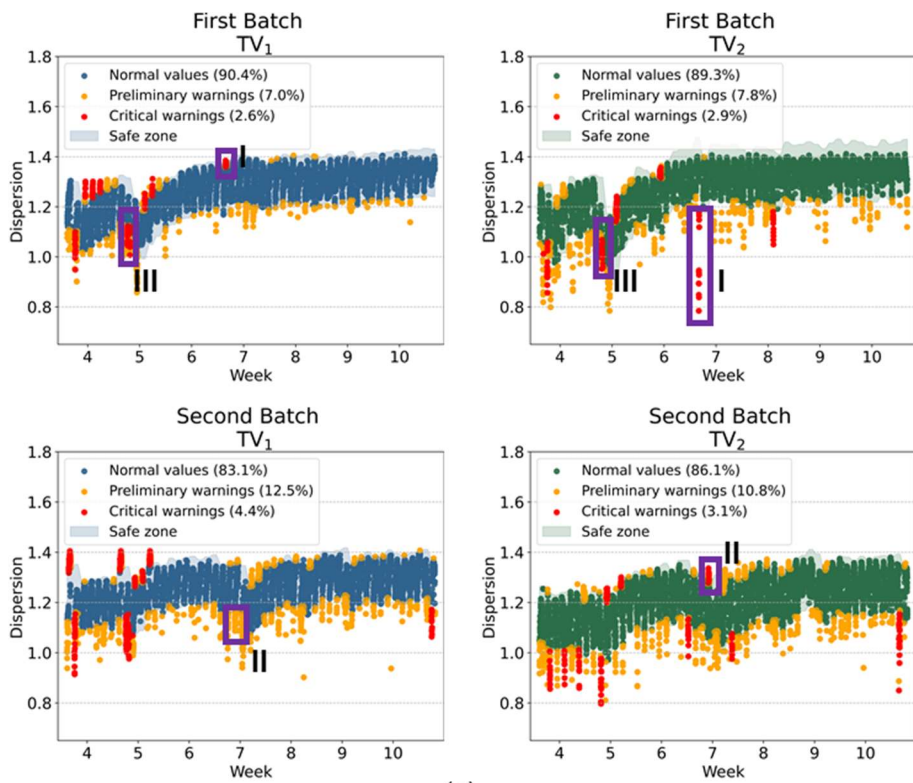
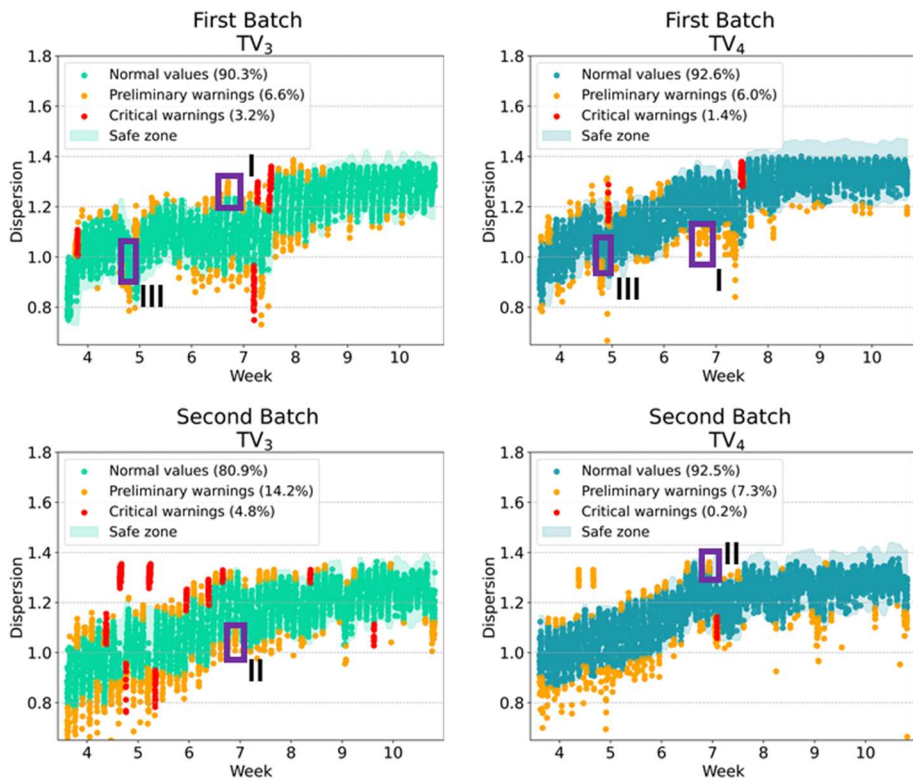


Figure 4.10 OB behavior in (a) Region 1 and (b) Region 2. The Roman numerals indicate cases to be discussed.

Chicken dispersion was modeled using ARIMA and anomalous dispersion values were detected (Figure 4.11). The ARIMA model achieved an overall mean absolute percentage error (MAPE; De Myttenaere et al., 2016) of 3.44%, indicating that the proposed approach successfully described the change in chicken dispersion along the growth of the chickens. In the first batch, 14 and 7 critical warning events, respectively, occurred in Region 1 and Region 2. In the second batch, 18 and 11 critical warning events occurred in Region 1 and Region 2, respectively.



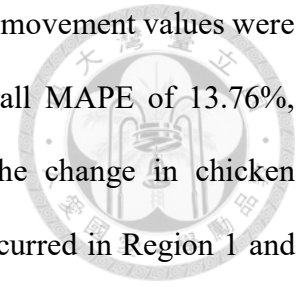
(a)

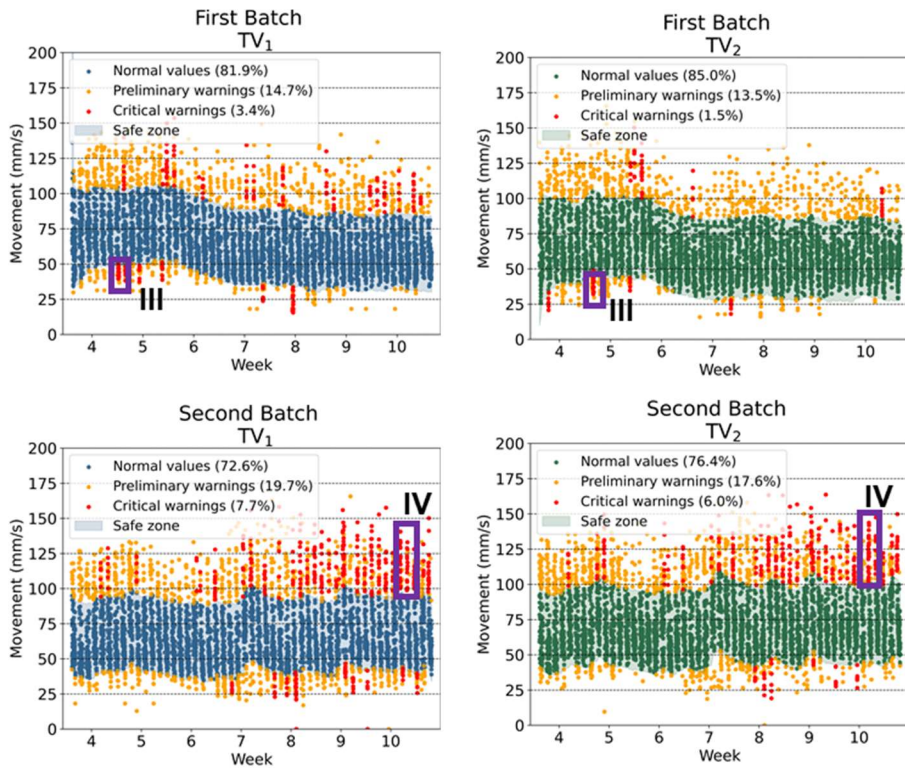
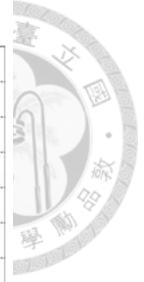


(b)

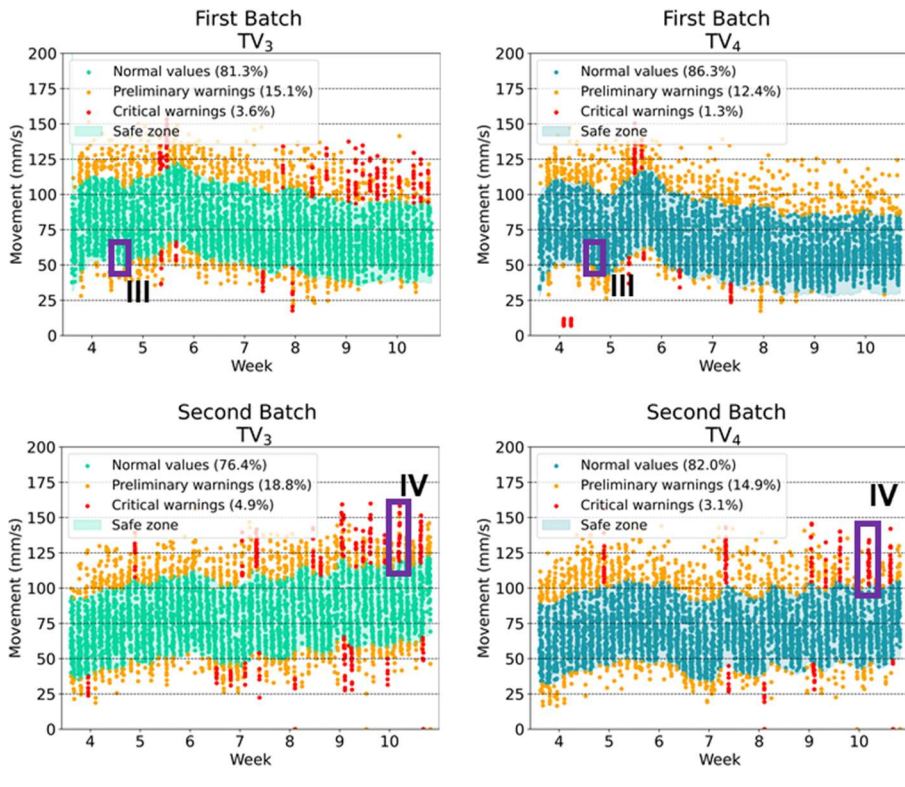
Figure 4.11 Chicken dispersion in (a) Region 1 and (b) Region 2. The Roman numerals indicate cases to be discussed.

Chicken movement was modeled using SARIMAX and anomalous movement values were detected (Figure 4.12). The SARIMAX model achieved an overall MAPE of 13.76%, indicating that the proposed approach successfully described the change in chicken movement. In the first batch, 29 and 27 critical warning events occurred in Region 1 and Region 2, respectively. In the second batch, 67 and 33 critical warning events, respectively, occurred in Region 1 and Region 2. Notably, Region 1 had the highest number of critical warning events in movement during the second batch, most of which surpassed the predicted safe zone. This observation implies that Region 1 potentially experienced a higher frequency of disturbances than Region 2.





(a)



(b)

Figure 4.12 Chicken movement in (a) Region 1 and (b) Region 2. The Roman numerals indicate cases to be discussed.

Four anomalous events in OB behaviors, dispersion value, and movement value were discussed: (I) unusually in the western region of the chicken house, (II) unusually in the eastern region of the chicken house, (III) a sudden decrease in temperature, and (IV) unusually movement values. Event (I) occurred on June 20, 2022, between 16:30 and 17:30 (Figure 4.13). Anomalous dispersion values and OB ratios were observed. At the moment, the western regions of the chicken house (i.e., TV₂ and TV₄) were directly exposed to sunlight. Chickens migrated to the eastern regions, seeking shelter from intense sunlight and heat. Consequently, the mean dispersion values of TV₂ (0.78) and TV₄ (1.09), respectively, in the western region fell in the critical-warning and preliminary-warning zones of low dispersion value. By contrast, the mean dispersion values of TV₁ (1.38) and TV₃ (1.23), respectively, in the eastern region fell in the critical-warning and preliminary-warning zones of high dispersion value. Moreover, due to a mean temperature of 34.4°C and high dispersion values lasting for an hour in TV₁, a mean OB ratio in SV₁ reached 85.72%, falling in the critical-warning zone. By contrast, due to high dispersion values lasting for 30 min in TV₃, the mean OB ratio in SV₂ (72.36%) below to the threshold.

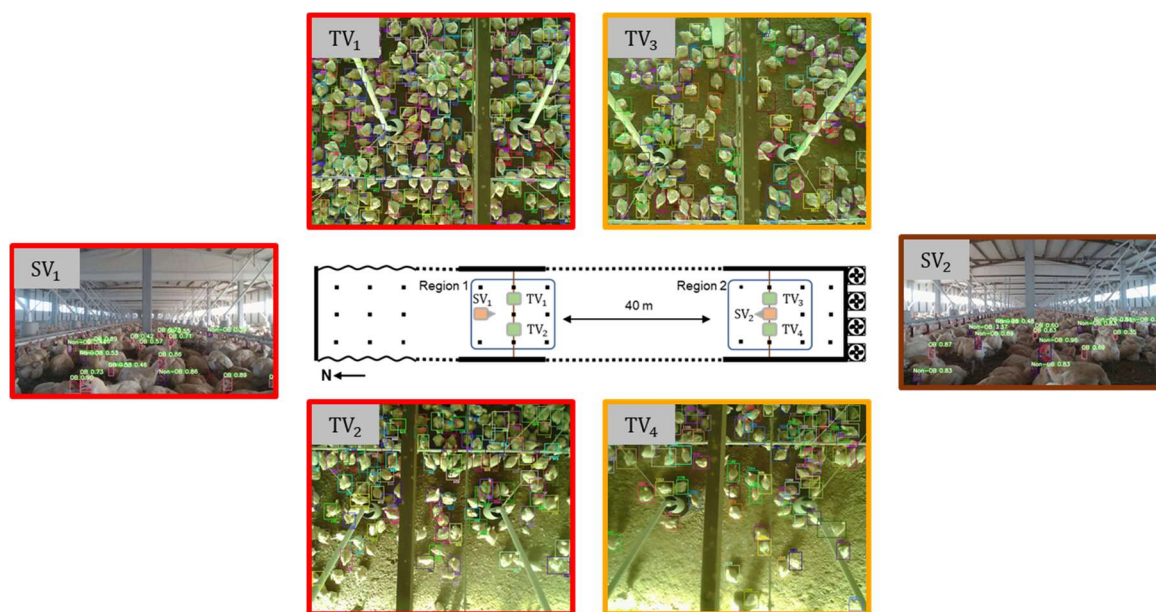


Figure 4.13 The top-view and side-view images in event (I) occurred on June 20, 2022, between 16:30 and 17:30.

Event (II) occurred on October 9, 2022, between 6:30 and 7:00 (Figure 4.14). At the time, the eastern regions of the chicken house (i.e., TV₁ and TV₃) were directly exposed to sunlight. Chickens migrated to the western regions, seeking shelter from intense sunlight and heat. Consequently, the mean dispersion values of TV₁ (1.11) and TV₃ (1.07) in the eastern region fell in the preliminary-warning zones of low dispersion value. By contrast, the mean dispersion values of TV₂ (1.26) and TV₄ (1.32), respectively, in the western region fell in the critical-warning and preliminary-warning zones of high dispersion value. Despite the crowding of chickens in TV₂ and TV₄, the OB ratios (SV₁: 47.58% and SV₂: 42.04%) remained below the threshold (i.e., 80.24%) owing to the temperature of 25.2°C.

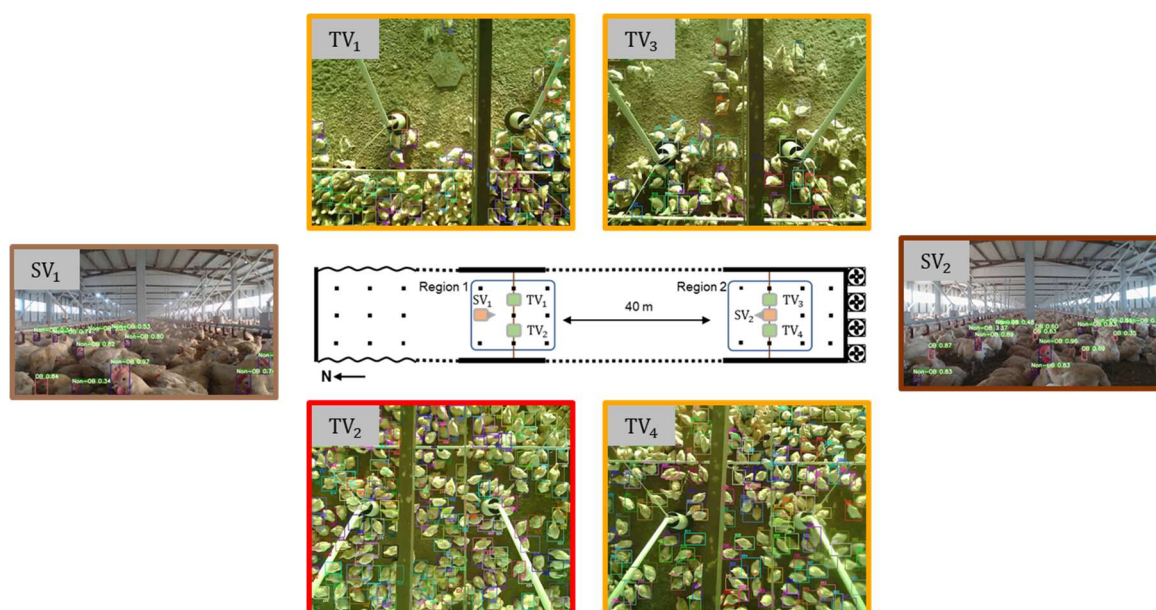


Figure 4.14 The top-view and side-view images in event (II) occurred on October 9, 2022, between 6:30 and 7:00.

Event (III) occurred June 7, 2022, at 16:00. Low dispersion values and movement values were observed. At the moment, a sudden decrease in temperature occurred. The recorded temperature dropped from 31.6°C at 11:00 to 26.6°C at 16:00. At 11:00, both the dispersion values (TV₁: 1.06, TV₂: 1.11, TV₃: 1.04, and TV₄: 1.09) and movement values (TV₁: 68.94 mm/s, TV₂: 54.29 mm/s, TV₃: 69.51 mm/s, and TV₄: 55.92 mm/s) in the two regions were

within the predicted safe zone (Figure 4.15a). Right after the temperature drop at 16:00, the chickens in Region 1 appeared to gather closely together (Figure 4.15b), resulting in low dispersion (TV_1 : 1.01 and TV_2 : 0.95) and movement (TV_1 : 31.12 mm/s and TV_2 : 41.65 mm/s). By contrast, despite the sudden drop in temperature, the dispersion (TV_3 : 1.05 and TV_4 : 1.07) and movement (TV_3 : 55.18 mm/s and TV_4 : 57.57 mm/s) observed in Region 2 remained in the predicted safe zone. The chickens in Region 2 appeared to gather around the feeding buckets and consume the provided feed. This discrepancy might suggest the possibility that the chicken in Region 1 were more susceptible to temperature changes.

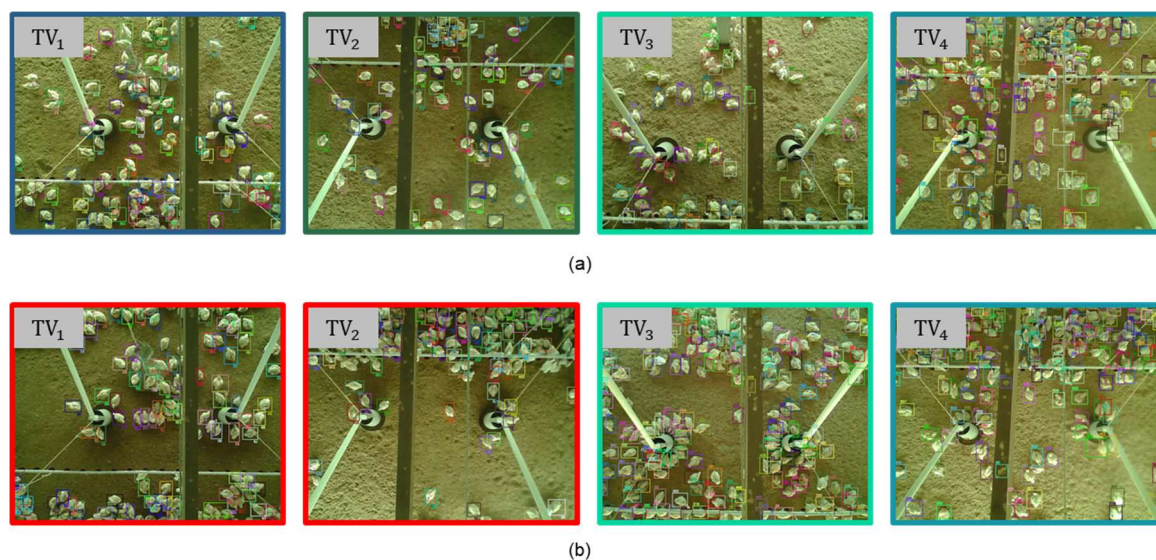


Figure 4.15 The top-view images in event (III) occurred on (a) June 7, 2022, at 11:00 and (b) at 16:00.

Event (IV) occurred on November 1, 2022, between 6:30 and 10:30. At the moment, flocks of chickens moved consistently for 3 hours within the field of the camera, resulting in mean movement values of 122.34 mm/s, 122.86 mm/s, 124.32 mm/s, and 110.28 mm/s per chicken in the TV_1 , TV_2 , TV_3 , and TV_4 , respectively (Figure 4.16). By contrast, the overall mean movement value of the second batch was 66.46 mm/s, 72.52 mm/s, 81.09 mm/s, and 71.66 mm/s per chicken in the TV_1 , TV_2 , TV_3 , and TV_4 , respectively. The underlying reasons for the extreme high movement values remain unknown, necessitating further

investigation. However, this observation indicates that the proposed approach of observing chicken movement is effective.

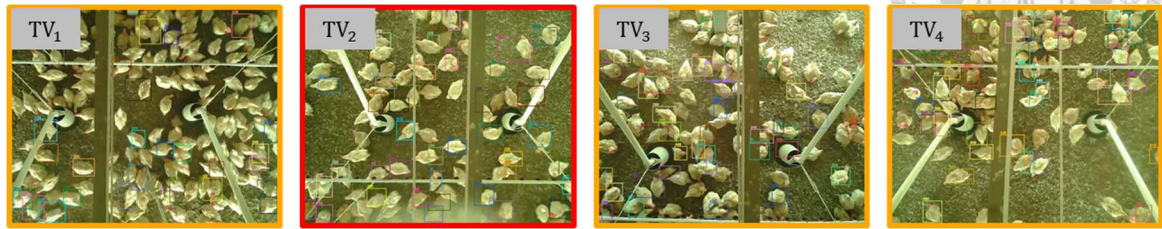
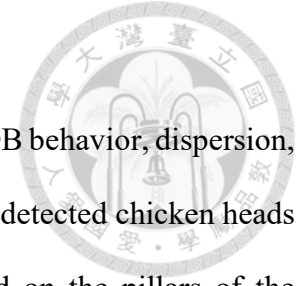


Figure 4.16 The top-view images in event (IV) occurred on (a) November 1, 2022, between 6:30 and 10:30.

CHAPTER 5 CONCLUSION



This study proposes an approach for automatically quantifying the OB behavior, dispersion, and movement of TNCs in commercial chicken farms. The OBDM detected chicken heads in the side-view videos, acquired by embedded systems installed on the pillars of the chicken house, and quantified the ratio of the chickens with OB behaviors (also referred to as OB ratio). The CDTM localized chickens in the top-view videos, acquired by embedded systems installed on the beams of the chicken house, tracked the chickens and quantified spatial dispersion and movement of the chickens using NN and Bytetrack algorithm, respectively. The safe zones of OB ratio, dispersion, and movement, respectively, were determined using mean and standard deviation, 95% confidence intervals of ARIMA, and 95% confidence intervals SARIMAX. The values outside the safe zones were considered as warnings. OBDM achieved an overall mAP of 91.3% in chicken head detection. CDTM achieved a mAP of 95.8% in chicken localization. CDTM achieved an overall MOTA of 89.5% in chicken tracking. The ARIMA and SARIMAX models, respectively, achieved a MAPE of 3.44% and 13.76%, indicating that the proposed approach successfully described the change in dispersion and movement. The proposed approach is objective and automated, potentially mitigating the necessity for manual patrols by chicken farmers in chicken farms.

REFERENCE



- Agricultural Statistics Yearbook*. (2021). Council of Agriculture, Executive Yuan, Taiwan
- Animal and Plant Epidemics*. (2023).
- Aydin, A., Cangar, O., Ozcan, S. E., Bahr, C., & Berckmans, D. (2010). Application of a fully automatic analysis tool to assess the activity of broiler chickens with different gait scores. *Computers and Electronics in Agriculture*, 73(2), 194-199.
- Bewley, A., Ge, Z., Ott, L., Ramos, F., & Upcroft, B. (2016). Simple online and realtime tracking. 2016 IEEE international conference on image processing (ICIP),
- Bochkovskiy, A., Wang, C.-Y., & Hong, Y. (2020). YOLOv4: Optimal Speed and Accuracy of Object Detection. *arXiv pre-print server*. <https://doi.org/None>
arxiv:2004.10934
- Bottou, L. (2012). Stochastic gradient descent tricks. *Neural Networks: Tricks of the Trade: Second Edition*, 421-436.
- Box, G. E., Jenkins, G. M., Reinsel, G. C., & Ljung, G. M. (2015). *Time series analysis: forecasting and control*. John Wiley & Sons.
- Clark, P. J., & Evans, F. C. (1954). Distance to nearest neighbor as a measure of spatial relationships in populations. *Ecology*, 35(34), 445-453.
- Darkpgmr. (2020). *Dark label*. <https://github.com/darkpgmr/DarkLabel>
- De Myttenaere, A., Golden, B., Le Grand, B., & Rossi, F. (2016). Mean absolute percentage error for regression models. *Neurocomputing*, 192, 38-48.
- Everingham, M., Van Gool, L., Williams, C. K. I., Winn, J., & Zisserman, A. (2010). The Pascal Visual Object Classes (VOC) Challenge. *International Journal of Computer Vision*, 88(2), 303-338. <https://doi.org/10.1007/s11263-009-0275-4>
- FAOSTAT. (2022). *Food and Agriculture Organization of the United Nations*. FAOSTAT. <http://www.fao.org/faostat/en/?#data>
- Fawcett, T. (2006). An introduction to ROC analysis. *Pattern Recognition Letters*, 27(8), 861-874. <https://doi.org/10.1016/j.patrec.2005.10.010>
- Guo, Y., Aggrey, S. E., Wang, P., Oladeinde, A., & Chai, L. (2022). Monitoring Behaviors of Broiler Chickens at Different Ages with Deep Learning. *Animals*, 12(23), 3390. <https://doi.org/10.3390/ani12233390>
- Heartex. (2015). *LabelImg*. <https://github.com/heartexlabs/labelImg>
- Jiang, P., Ergu, D., Liu, F., Cai, Y., & Ma, B. (2022). A Review of Yolo algorithm developments. *Procedia Computer Science*, 199, 1066-1073.
- Kalman, R. E. (1960). A new approach to linear filtering and prediction problems.
- Kashiha, M., Pluk, A., Bahr, C., Vranken, E., & Berckmans, D. (2013). Development of an early warning system for a broiler house using computer vision. *Biosystems Engineering*, 116(1), 36-45. <https://doi.org/10.1016/j.biosystemseng.2013.06.004>

- Kuhn, H. W. (1955). The Hungarian method for the assignment problem. *Naval research logistics quarterly*, 2(1-2), 83-97.
- Lee, S., & Lee, D. K. (2018). What is the proper way to apply the multiple comparison test? *Korean journal of anesthesiology*, 71(5), 353-360.
- Lin, C.-Y., Hsieh, K.-W., Tsai, Y.-C., & Kuo, Y.-F. (2020). Automatic Monitoring of Chicken Movement and Drinking Time Using Convolutional Neural Networks. *Transactions of the ASABE*, 63(6), 2029-2038. <https://doi.org/10.13031/trans.13607>
- Lott, B., Simmons, J., & May, J. (1998). Air velocity and high temperature effects on broiler performance. *Poultry science*, 77(3), 391-393.
- Manning, C., & Schutze, H. (1999). *Foundations of statistical natural language processing*. MIT press.
- Milan, A., Leal-Taixé, L., Reid, I., Roth, S., & Schindler, K. (2016). MOT16: A benchmark for multi-object tracking. *arXiv preprint arXiv:1603.00831*.
- Mirjalili, S., & Mirjalili, S. (2019). Genetic algorithm. *Evolutionary Algorithms and Neural Networks: Theory and Applications*, 43-55.
- Neethirajan, S. (2022). ChickTrack—a quantitative tracking tool for measuring chicken activity. *Measurement*, 191, 110819.
- Pereira, D. F., Miyamoto, B. C., Maia, G. D., Sales, G. T., Magalhães, M. M., & Gates, R. S. (2013). Machine vision to identify broiler breeder behavior. *Computers and Electronics in Agriculture*, 99, 194-199.
- Purswell, J. L., Dozier III, W. A., Olanrewaju, H. A., Davis, J. D., Xin, H., & Gates, R. S. (2012). Effect of temperature-humidity index on live performance in broiler chickens grown from 49 to 63 days of age. 2012 IX International Livestock Environment Symposium (ILES IX),
- Siriani, A. L. R., Kodaira, V., Mehdizadeh, S. A., De Alencar Nääs, I., De Moura, D. J., & Pereira, D. F. (2022). Detection and tracking of chickens in low-light images using YOLO network and Kalman filter. *Neural Computing and Applications*, 34(24), 21987-21997. <https://doi.org/10.1007/s00521-022-07664-w>
- Statistical Illustration of Livestock Husbandry*. (2021).
- Sun, Q., Wu, T., Zou, X., Qiu, X., Yao, H., Zhang, S., & Wei, Y. (2019). Multiple object tracking for yellow feather broilers based on foreground detection and deep learning. *INMATEH-Agricultural Engineering*(2).
- Wang, C.-Y., Bochkovskiy, A., & Hong, Y. (2022). YOLOv7: Trainable bag-of-freebies sets new state-of-the-art for real-time object detectors. *arXiv pre-print server*. <https://doi.org/None>
- arxiv:2207.02696
- Wojke, N., Bewley, A., & Paulus, D. (2017). Simple online and realtime tracking with a deep association metric. 2017 IEEE international conference on image processing (ICIP),

- Yu, Z., Liu, L., Jiao, H., Chen, J., Chen, Z., Song, Z., Lin, H., & Tian, F. (2022). Leveraging SOLOv2 model to detect heat stress of poultry in complex environments. *Frontiers in Veterinary Science*, 9.
- Zhang, Y., Sun, P., Jiang, Y., Yu, D., Weng, F., Yuan, Z., Luo, P., Liu, W., & Wang, X. (2022). ByteTrack: Multi-object Tracking by Associating Every Detection Box. In *Computer Vision–ECCV 2022: 17th European Conference* (pp. 1-21). Springer Nature Switzerland. https://doi.org/10.1007/978-3-031-20047-2_1
- Zhu, X., Wu, C., Yang, Y., Yao, Y., & Wu, Y. (2022, 2022). Automated Chicken Counting Using YOLO-v5x Algorithm.
- Zhuang, X., Bi, M., Guo, J., Wu, S., & Zhang, T. (2018). Development of an early warning algorithm to detect sick broilers. *Computers and Electronics in Agriculture*, 144, 102-113.
- Zhuang, X., & Zhang, T. (2019). Detection of sick broilers by digital image processing and deep learning. *Biosystems Engineering*, 179, 106-116.